Optical and electrical studies of ZnO thin films heavily implanted with silver ions



2014 J. Phys.: Conf. Ser. 572 012022

(http://iopscience.iop.org/1742-6596/572/1/012022)

Journal of Physics: Conference Series **572** (2014) 012022 doi:10.1088/1742-6596/572/1/012022

# Optical and electrical studies of ZnO thin films heavily implanted with silver ions

**N M Lyadov[1*,2], A I Gumarov[2], V F Valeev[1], V I Nuzhdin[1], R I Khaibullin[1,2], and I A Faizrakhmanov[1,2]**

[1] Zavoisky Physical-Technical Institute of Russian Academy of Sciences, Sibirsky Tract 10/7, Kazan 420029, Russia
[2] Department of Physics, Kazan Federal University, Kremlyovskaya st. 18, Kazan 420008, Russia

*E-mail: nik061287@mail.ru

**Abstract**. Thin films of zinc oxide (ZnO) with the thickness of 200 nm have been deposited on quartz substrates by using ion-beam sputtering technique. Then Ag+ ions with the energy of 30 keV have been implanted into as-deposited ZnO films to the fluences in the range of $(0.25–1.00)\times10^{17}$ ions/cm$^2$ to form ZnO:Ag composite layers with different concentrations of the silver impurity. The analysis of the microstructure has shown that the thickness of the ZnO film decreases, and the Ag dopant concentration tends to the saturation with increasing Ag implantation fluence. The ZnO:Ag composite layers reveal the optical selective absorption at the wavelength of the surface plasmon resonance that is typical for silver nanoparticles dispersed in the ZnO matrix. The red shift of the plasmon resonance peak from 480 to 500 nm is observed with the increase in the implantation fluence to $0.75\times10^{17}$ Ag ions/cm$^2$. Then the absorption peak position starts the backward motion, and the absorption intensity decreases with the subsequent increase in the implantation fluence. The non-monotonic dependence of the absorption peak position on the implantation fluence has been analyzed within of Maxwell Garnet theory and taking into account the strong sputtering of ZnO films during implantation. The ZnO:Ag composite layers exhibit the p-type conductivity indicating that a part of $Ag^+$ ions is in the form of acceptor impurities implanted into the ZnO lattice.

## 1. Introduction

Zinc oxide (ZnO) is a direct-gap semiconductor with the band gap of 3.4 eV. This oxide semiconductor has many attractive properties, in particular the high exciton binding energy of ~ 60 meV at room temperature, which makes it promising for creating ultraviolet LEDs, lasers, photosensors, piezoelectric and transparent electrodes, etc. [1,2]. On the other hand, nanocomposite materials based on the dispersion of metal nanoparticles in optical transparent semiconductors are the objects of intensive studies for over the last 20 years. Depending on the kind of metal nanoparticles these nanocomposite materials have important magnetic, optical, non-linear optical or catalytic properties for applications [3]. A special place is occupied by dispersion systems with nanoparticles of noble metals such as Cu, Ag and Au, which exhibit selective surface plasmon resonance (SPR) absorption in the visible and near infrared region. These unique properties of the plasmon-active particles of noble metals cause a number of new physical effects in the composite semiconductors, such as section increase in Raman scattering, the strong increase in light emitting structures efficiency, etc. [4].

It is well known that usually semiconductor ZnO thin films and bulk crystals reveal the n-type conductivity which is caused either by oxygen vacancies or Zn interstitial atoms being electron donors in the ZnO lattice. However, one of the basic problems of semiconductor optoelectronics based on the ZnO material consists in the production of the ZnO material with the stable p-type conductivity and sufficiently high optical transparency. Silver or nitrogen is the most intensively studied acceptor impurity, using which many authors already obtained the p-type conductivity in ZnO using different methods [1, 5]. In this work we used high-fluence implantation with $Ag^+$ ions into ZnO films to form p-type ZnO:Ag composite layers with silver metal nanoparticles. The influence of the implantation fluence on the structural, optical and electric properties of the Ag-implanted ZnO films was studied by using scanning electron microscopy with elemental microanalysis, optical spectroscopy, as well as dc electric resistance, Hall and Seebeck effect measurements at room temperature.

## 2. Experimental

ZnO thin films were deposited on the quartz substrate ($SiO_2$) by ion-beam sputtering of the zinc metal target (purity: 99.99 %) in oxygen atmosphere. Chemically pure xenon (Xe) as a working gas was used in the sputtering procedure. The energy of $Xe^+$ ions was 1 keV, and the ion beam current density was 100 μA/cm$^2$ during sputtering of the zinc target for 30 min.. Then $Ag^+$ ions with the energy of 30 keV were implanted into as-deposited ZnO films to high fluences in the range of $(0.25 - 1.00)\times10^{17}$ ions/cm$^2$ to form composite ZnO layers with different concentrations of silver impurity. The Ag implantation was carried out in ZnO films at room temperature on an *ILU-3* ion-beam accelerator (Zavoisky Physical-Technical Institute, Kazan). Some as-prepared samples were subjected to thermal annealing for 15 min in vacuum ($10^{-6}$ Torr) or in air at the temperatures ranging from 500 to 1000 K.

The measurements of the ZnO film thickness before and after ion implantation, as well the analysis of the surface morphology and elemental composition of samples under study were performed on an *EVO 50 XVP* scanning electron microscope (SEM) (*Carl Zeiss)* equipped with an *INCA Energy-350* elemental analyzer (*Oxford Instruments)*. Optical spectra were measured on a *Hitachi-330* dual-beam spectrophotometer in the wavelength range of 200 – 700 nm. The standard van der Pauw geometry was used in the measurement of the electrical resistivity, Hall and Seebeek parameters of as-deposited and implanted ZnO films. All above physical measurements were performed at room temperature.

## 3. Results and discussion

Figure 1 shows cross-section SEM images of as-deposited ZnO film and the same film implanted with $Ag^+$ ions to the fluence of $1.0\times10^{17}$ ions/cm$^2$. It is seen clearly that the initial film thickness is 215 nm, and it decreases to 165 nm due to strong sputtering of the ZnO film after high-fluence implantation. These values of the film thickness before and after silver ion implantation was used to estimate the sputtering coefficient as $S \cong 4$ atom/ion with allowance for the ZnO atomic density of $8.28\times10^{22}$ at/cm$^3$ and the fluence value.

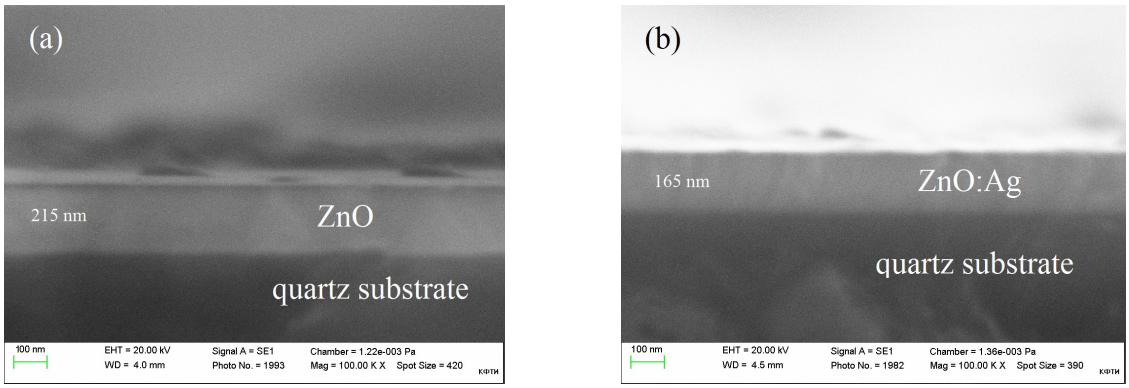


**Figure 1.** Cross section SEM images: (a) – as-deposited ZnO film, (b) – the same film implanted with $Ag^+$ ions to the fluence of $1.0\times10^{17}$ ions/cm$^2$.

The analysis of in-plane SEM images of ZnO thin films shows that all samples have a homogeneous and smooth surface before and after ion implantation. Table 1 presents the elemental composition of the samples under study. It shows the presence of implanted silver, and zinc and oxygen, elements forming the ZnO structure. Since the probing depth of 20 keV electrons in the microanalysis is on the order of 1 μm, the high silicon and oxygen concentration is due to the quartz substrate ($SiO_2$), and the low Ag content is induced by the averaging over the full depth probing of the electron beam.

**Table 1.** Elemental composition of as-deposited and Ag-implanted ZnO thin films.

| Sample | Fluence (ion/cm$^2$) | Composition (at.%) | | | |
|---|---|---|---|---|---|
| | | O ($K_\alpha$) | Si ($K_\alpha$) | Zn ($K_\alpha$) | Ag ($K_\alpha$) |
| ZnO as-deposited | | 56.1 | 28.2 | 15.7 | |
| ZnO:Ag(1) | $0.25\times10^{17}$ | 55.3 | 29.0 | 15.3 | 0.4 |
| ZnO:Ag(2) | $0.50\times10^{17}$ | 54.7 | 29.4 | 15.1 | 0.8 |
| ZnO:Ag(3) | $0.75\times10^{17}$ | 54.1 | 31.2 | 14.9 | 0.8 |
| ZnO:Ag(4) | $1.00\times10^{17}$ | 53.6 | 31.4 | 14.2 | 0.8 |

Depth profiles of the silver concentration were calculated using the *SRIM-2008* simulation code [6]. We used the formula 11 from [7] to take into account the surface sputtering of ZnO with the above coefficient S = 4 atom/ion during implantation. The calculated profiles of the silver concentration in ZnO films implanted to different fluences are shown in figure 2. According to SRIM calculations, the mean range ($R_p$) of 30 keV Ag ions is about 12.1 nm with a straggling ($\Delta R_p$) of 4.8 nm in the Gaussian-like depth distribution. Thus, the real thickness of the modified ZnO layer amounts to (Rp +2$\Delta$Rp) ~ 20-25 nm. The shape of the implantation profile initially changes with the fluence due to surface sputtering. The profile shape becomes smooth and the peak of Ag concentration shifts to the surface with increasing fluence. Our calculations and EDS elemental microanalysis show that the silver concentration increases with increasing fluence, and it tends to the saturation nominally reaching 25 at % in the peak of the depth profile for the highest fluence of $1.0\times10^{17}$ ion/cm$^2$. Such high concentration of the doping impurity leads to its precipitation in the form of Ag nanoparticles.

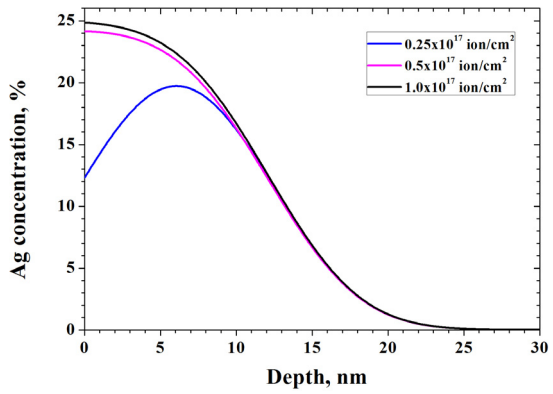


**Figure 2.** The depth profiles of silver concentration in ZnO films implanted with $Ag^+$ ions to different fluences.

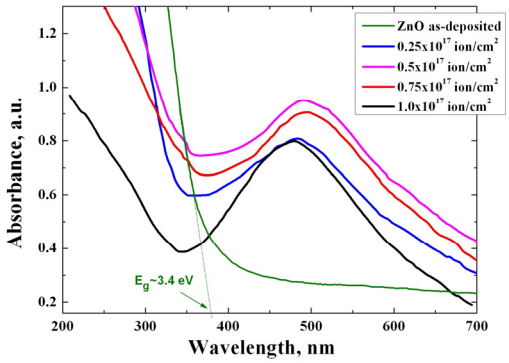


**Figure 3.** Optical absorption spectra of as-deposited ZnO film and ZnO films implanted with $Ag^+$ ions to different fluences.

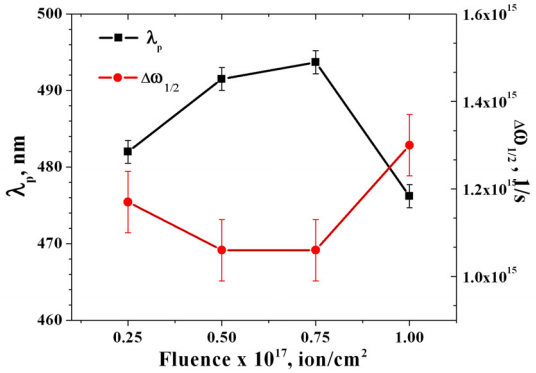


**Figure 4.** Fluence dependencies of peak position ($\lambda_p$) and half-width ($\Delta\omega_{1/2}$) of plasmon resonance in Ag-implanted ZnO films.

The formation of silver nanoparticles in Ag-implanted ZnO films was confirmed by optical absorption spectroscopy. Figure 3 shows the changes in optical absorption spectra of ZnO films after Ag ion implantation at different fluences. It can be seen that the selective absorption is observed at the wavelength $\lambda_p \cong 482$ nm in the sample implanted at low fluence $0.25\times10^{17}$ ions/cm$^2$. The absorption increases in intensity and shifts toward longer wavelengths for large fluence values. Then the absorption peak starts the backward motion, and the absorption intensity decreases in the ZnO film implanted to the highest fluence of $1.0\times10^{17}$ ions/cm$^2$. The observed selective absorption is attributed to the surface plasmon resonance (SPR) in the small silver particles because the dispersed isolated Ag ions or atoms do not exhibit such resonance absorption.

The dependences of the peak position ($\lambda_p$) and half-width ($\Delta\omega_{1/2}$) of plasmon resonance on the implantation fluence in Ag-implanted ZnO films are shown in figure 4. The experimental dependences are not monotonic and have a maximum for the peak position and a minimum for the half-width at the fluence of $0.75\times10^{17}$ ion/cm$^2$. Note that similar fluence dependences were observed earlier in the polymers heavily implanted with 30 keV $Ag^+$ ions [8, 9]. It was shown that non-monotonic behavior of the SPR peak position versus the implantation fluence originates from the transformation size of silver nanoparticles and their agglomeration at high fluences. In fact, the peak position and absorption bandwidth depend on the size of silver nanoparticles according to both well-known Mie and Maxwell Garnett theories with allowance for the size-dependent collision frequency in metal particles [10, 11]. In particular, we used the bandwidth at half-maximum absorption (half-width) to estimate silver particle dimensions in the implanted ZnO films by using formula [10]:

$$R = \frac{\upsilon_F}{\Delta\omega_{1/2}} \qquad (1),$$

where $R$ is the radius of spherical particles formed in the Ag-implanted ZnO film, $\Delta\omega_{1/2}$ are experimental values of the absorption half-width, and $\upsilon_F = 1.4\times10^6$ m/s is the Fermi velocity for the electron in silver. According to our calculations, the decrease in the half-width indicate the increase in the mean size of nanoparticles from 2.4 to 2.7 nm in the fluence range $(0.25 \text{ to } 0.75)\times10^{17}$ with the subsequent decrease to 2.2 nm as the fluence is increased to $1.0\times10^{17}$ ions/cm$^2$. This non-monotonic change of the nanoparticle size with increasing fluence can be understood by taking into account the non-uniform depth distribution of the implanted silver and strong sputtering of ZnO films during implantation. The Gaussian-like shapes of Ag concentration curves (fig.2) allow an assumption that there is a wide size distribution of the forming particle over the depth of the implanted region. This means that the high concentration of the Ag impurity in the peak of the distribution stimulates the

growth of silver nanoparticles with larger sizes in the near-surface region, whereas the lower density of Ag atoms in the tail of the concentration curve contributes to the nucleation of smaller size clusters that dominate at the depth of the ZnO film. At the first stage, the sizes of large and small silver particles increase with increasing fluence to $0.75\times10^{17}$ ions/cm$^2$ as it is seen from our calculations. These silver nanoparticles move steadily toward the surface due to sputtering of the ZnO film. At fluences above $0.75\times10^{17}$ ions/cm$^2$, the nanoparticles with large sizes come to the surface and disappear due to the apparent loss of Ag from the sample surface during its sputtering. The latter results in the decrease in the mean size of silver nanoparticles and the overall optical absorption decreases, as it takes place in the sample implanted to the highest fluence of $1.0\times10^{17}$ ions/cm$^2$.

According to calculations [11] obtained using the Mie theory, the position of the maximum of the extinction coefficient is almost independent of the size of silver particles in radius range of 1-10 nm, while in the experiment we observe a noticeable shift of the absorption maximum (fig. 4). However, the Mie theory is valid only for low concentrations of metal particles in dielectric matrix. In our case, the Maxwell Garnett theory [12] is more appropriate, according to which the peak position of the maximum absorption is determined principally by the filling factor ($Q$) of metal nanoparticles in ZnO matrix as:

$$\left|\varepsilon_1(\lambda_p)\right| = \frac{(2+Q)}{(1-Q)} n(\lambda_p)_s^2 \qquad (2),$$

where $\varepsilon_1(\lambda_p)$ is real part of the complex dielectric function of the silver at the wavelength $\lambda_p$ corresponding to the maximum of the plasmon resonance absorption at a given implantation fluence, and $n_s$ is refractive index of ZnO film (here $n_s \cong 1.98$ at plasmon resonance wavelength). According to formula (2), the experimental red shift of the absorption maximum is induced by the increase in the filling factor from f≅0.05 to 0.1 with increasing implantation fluence of silver. The backshift in short-wave region for highest fluence of $1.0\times10^{17}$ ions/cm$^2$ is probably due either a decrease in the refractive index of the implanted ZnO film or the apparent loss of Ag metal from the sample during its sputtering as it was above described.

Table 2 presents the results of electrical measurements in as-deposited ZnO films and the same films implanted with $Ag^+$ ions to the fluence of $0.25\times10^{17}$ ions/cm$^2$. As expected, initial deposited ZnO films reveal the n-type conductivity and have the low specific resistance (~$10^{-3}$ Ohm·cm) due to the high value of the free electron concentration (~$10^{20}$ cm$^{-3}$) in the ZnO conduction band. The high carrier concentration in semiconductor oxides, such as ZnO, CuO, $TiO_2$ etc., usually caused by the low oxygen content in the stoichiometric composition of oxide materials. In fact, subsequent annealing of as-deposited ZnO films in the reducing environment of air at 1000 K leads to the recovery of stoichiometry and the huge decrease in electric conductivity. The annealed ZnO films exhibit the high-resistance behavior at room temperature in the absence of the doping impurity.

**Table 2.** Electrical parameters of as-deposited ZnO film and the same film implanted with $Ag^+$ ions to the fluence of $0.25\times10^{17}$ ions/cm$^2$.

| Sample | Type of conductivity | Carrier mobility (cm$^2$/V·s) | Carrier concentration (cm$^{-3}$) | Specific resistance (Ohm·cm) |
|---|---|---|---|---|
| ZnO as-deposited | n | 9.43 | $2.5\cdot10^{20}$ | $2.65\cdot10^{-3}$ |
| ZnO as-deposited, *after annealing in air at 1000 K* | - | - | - | high-resistance |
| ZnO:Ag (1), implanted | p | 1.2 | $2.8\cdot10^{16}$ | 220 |
| ZnO:Ag (1) implanted *after annealing in air at 1000 K* | - | - | - | high-resistance |
| ZnO:Ag (1), implanted *after one year of storage in air* | p | 1.2 | $2.8\cdot10^{16}$ | 220 |

High-fluence implantation with silver ions into as-deposited ZnO film also results in the significant increase in their specific resistance to the value about $10^2$ Ohm·cm. It is well known that ion implantation induces a large number of structural defects in the crystal lattice of the implanted material. Thus, the observed decrease in the electrical conductivity in Ag-implanted ZnO film can be caused by the formation of deep electron traps in the ZnO band gap. But more important is the fact that the type of conductivity of the ZnO film changes from n-type (by electrons) to p-type (by holes) after Ag ion implantation as it shows our Hall and Seebeek effect measurements. This means that a part of the $Ag^+$ ions is implanted into the ZnO lattice in the form of acceptor impurities. Note that the carrier mobility and concentration listed in Table 2 for Ag-implanted ZnO sample are very similar to the ones in p-type ZnO films doped homogeneously with Ag impurity [13]. Moreover, the measurements of the electrical properties with the time interval of 12 months showed the stable p-type conductivity in Ag-implanted ZnO films. It should be noted that the carrier concentration and the mobility of charge carriers in the sample were also unchanged. Annealing of Ag-implanted samples in air at temperatures above 500 K results in the high-resistance state of ZnO films. On the other hand, annealing in high vacuum at the same temperatures causes the complete evaporation of as-deposited and Ag-implanted films.

## 4. Conclusions

Our structural and optical studies show that high-fluence implantation with $Ag^+$ ions make it possible to synthesize silver nanoparticles in the surface region of the semiconductor ZnO matrix. The ion-synthesized silver nanoparticles reveal selective absorption at the wavelength of surface plasmon resonance in optical spectra of Ag-implanted ZnO films. It is established that the intensity and spectral position of surface plasmon resonance are strongly dependent on the implantation fluence. ZnO:Ag layers with silver metal nanoparticles exhibit the stable p-type electric conductivity that is important for practical applications of these composite materials.

## Acknowledgments

This study was supported by Russian Youth Scientific-Innovation Program “U.M.N.I.K.”.

## References

[1] Ozgur U, Alivov Ya I, Liu C, Teke A, Reshchikov M A, Dogan S, Avrutin V, Cho S.-J., Morkoc H 2005 *J. Appl. Phys.* **98** 041301
[2] Gorla C R, Emanetoglu N W, Liang S, Mayo W E, Lu Y et al. 1999 *J. Appl. Phys.* **85**(5) 2595
[3] Stepanov A L, Khaibullin I B 2005 *Rev. Adv. Mater. Sci.* № 9 109
[4] Maier S A 2007 *Plasmonics: Fundamentals and Applications, Springer Science* **XXV** 223 p.
[5] Sun F, Shan C X, Li B H, Zhang Z Z, Shen D Z, Zhang Z Y, and Fan D 2011 *Optics Letters* **36**(4) 499
[6] Ziegler J F, Biersack J P, Littmark U 1985 *The Stopping and Range of Ions in Solids* (Pergamon Press, New York) (*SRIM-2008* software at http://www.srim.org/)
[7] Achkeev A A, Khaibullin R I, Tagirov L R, Mackova A, Hnatowicz V, and Cherkashin N 2011 *Physics of Solid State* **53**(3) 543
[8] Khaibullin R I, Osin Y N, Stepanov A L, Khaibullin I B 1998 *Vacuum* **51** (2) 289
[9] Khaibullin R I, Osin Y N, Stepanov A L, Khaibullin I B 1999 *Nucl. Instr. and Meth. in Phys. Res.* **B 148** 1023
[10] Arnold G W 1975 *J. Appl. Phys.* **46**(10) 4466
[11] Arnold G W, Borders J A 1977 *J. Appl. Phys.* **48**(4) 1488
[12] Maxwell Garnett J.C., 1906 *Philos. Trans. R. Soc. Lond* **205** 237
[13] Duan L., Zhang W., Yu X., Wang P., Jiang Z., Luan L., Chen Y., Li D., 2013 *Solid State Commun.* **157** 45.